JONG-YEON HWANG[1], MYUNG JONG CHO[1], BRIAN G. THOMAS[2] AND SEONG-MOOK CHO[3]

NUMERICAL SIMULATION OF TURBULENT STEEL CEM® MOLD UNDER HIGH MASS FLOW CONDITION

Abstract

The POSCO CEM® (Compact Endless casting & rolling Mill) process can continuously produce coils without cutting before the finishing mill. A material balance with high throughput between the casting and rolling processses is essential to achieve this process. World-class throughput of CEM® has been achieved with high-speed casting technology (up to 8.0 m/min) and increased slab thickness (up to 100 mm). Many steel making companies are requiring that higher throughput casters should be manufactured for this kind of directly linked process. To accomplish this high throughput casting, many new advanced technologies are required and stability of the meniscus in the mold is one of the important factors. Electro Magnetic Braking (EMBr) system has come into the spotlight to control mold surface profile and level fluctuations. Therefore, an accurate evaluation and improvement of EMBr is required.

In this work, a numerical study was carried out to investigate high throughput conditions, to prepare for the next generation of CEM®. The slab thickness is 110mm with slab width 1,600 to 1,900mm. In order to effectively stabilize mold flow near the meniscus, a new SEN was designed, combined with a U-shaped EMBr invented by POSCO. This system was numerically evaluated for various external magnetic fields up to 0.35 T. Numerical results are consistently agreed with plant measurements obtained using nail board tests. A stabilized mold level is one of the critical technologies needed to achieve stable casting operation for high throughput operations.

Keywords

CEM®, Electromagnetic Brake (EMBr), Numerical Simulation, Mold Flow, SEN

1. Introduction

A new process, CEM® which can produce ultra-thin hot coils was launched by POSCO in 2009 [1]. As reported by Hwang et al., this process features 80~100 mm thick slabs directly going through a roughing mill located just after the caster, being reduced down to 20mm thickness, and then going into a small scale induction heater and finally being manufactured into ultra-thin coils through the hot finishing mill [1]. The coils are continuously produced without cutting before the finishing mill in this process, so is called endless rolling. Thin-gauge coils can be produced with uniform material quality due to consistent material temperature along the whole length of each strip. The mass balance between the caster and rolling mill is very important. Thus, high-throughput casting technology has to be accomplished because the capability of the hot rolling mill is greater than that of the caster. If casting speed is lower than a critical limit, heat loss during rolling part is increased, which leads to excessive rolling loads. Moreover, sufficient FM (Finishing Mill) coiling temperature has to be achieved for the grain structure of the coils not to become mixed. Therefore, the

[1] POSCO, [2] Colorado School of Mines, [3] Univ. Illinois

productivity of the caster in CEM® must be very high, compared to other casters. As shown in Fig. 1, the throughput per unit width of CEM® casters is the highest of all casting processes, including strip casters, thin slab casters, conventional casters and other ultra-thick slab casters. In addition, many producers desire increased production for other casters. Therefore, the stabilization of mold flow during high-speed casting operation is an important topic to investigate.

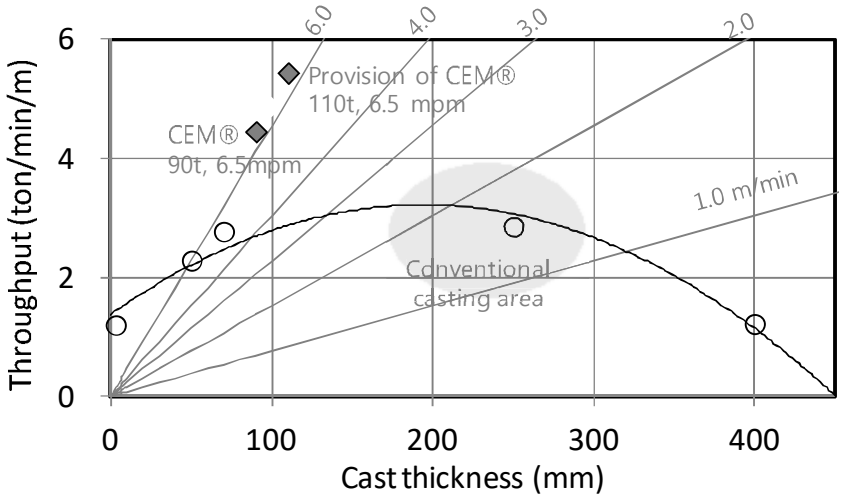

Fig. 1. Productivity related with cast thickness

Several investigations regarding this subject have been carried out in previous work. In particular, EMBr control of the flow fluctuations at the meniscus is known to improve the quality of the cast steel by reducing the penetration of non-metallic inclusions [2]. Three different EMBr configurations were studied: Local EMBr, EMBr Ruler, and FC Mold, as shown in Fig. 2 [3]. The nail board test is performed by dipping nails down through the slag layer and measuring the meniscus profile and velocity [3, 4]. The shape of the meniscus surface is also measured from oscillation mark profiles. Water modeling has difficulty to show the real flow of molten metal with EMBr in the mold [5]. Vogl et.al carried out not only numerical simulation but also experiments using the liquid metal GaInSn with a length scale of 1:8. It was reported that meniscus speed can be reduced from 0.2 to 0.09 m/sec with EMBr and a single SEN design combined with the installation of EMBr can offer new possibilities for extending the operational range. The transient fluid flow with argon gas was studied by nail board dipping test and Large Eddy Simulation (LES) coupled with the Lagrangian Discrete Phase Model (DPM) [6]. The dominant frequencies of jet flow were reported to be detected as 0.5-2.0Hz. Cho [7] investigated the effect of double-ruler EMBr on transient flow using a Reynolds Averaged Navier-Stokes (RANS) model coupled with Magnetohydrodynamics (MHD) and plant measurement using nail boards. The dominant frequency was observed at 0.03Hz. EMBr lowers the peaks in the level of power spectrum and decreases the level fluctuations near the SEN by 50%. LES is carried out with FC-Mold EMBr, which enables meniscus velocity to be decreased 0.5 to 0.3 m/sec and meniscus level to be reduced 12 to 1 mm [8]. Potential gradients in the Lorentz force term has to be discretized with great care along the boundary. Cho [9] developed a discretized method with second order accuracy, CIM, and showed good agreement with the analytical solution for plane channel flow.

In this study, numerical analysis of mold flow was performed for high throughput casting at 8.4-8.7 ton / min. This is 45% larger than that of CEM® currently in operation, 6 ton/min. A new SEN for high throughput was developed and applied to quantitatively evaluate the meniscus level and flow velocity.

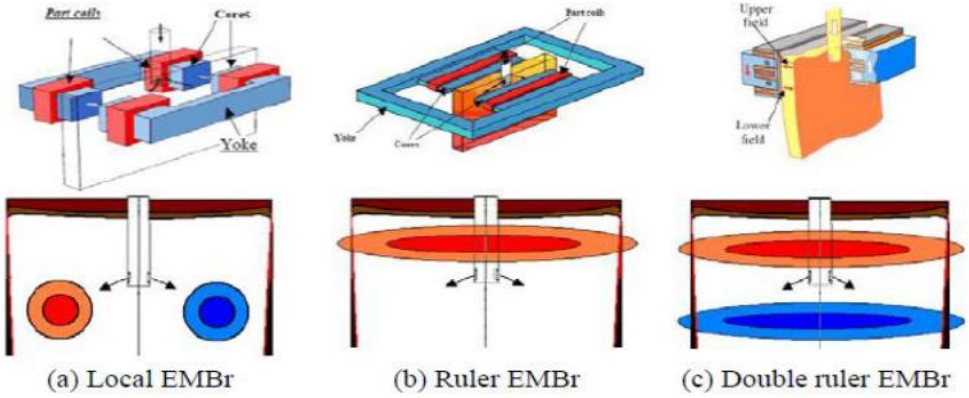

Fig. 2. Various type of EMBr [3]

2. Numerical Method and Flow Evaluation Criteria

The main numerical parameters are grid resolution, calculation domain and turbulence model. These parameters correlate strongly with computational reliability and cost. For turbulence modelling, the k-ε model is used with second order accuracy of spatial discretization. In order to guarantee a stable condition, an evaluation criterion is needed. Through long experience with CEM® performance, appropriate criteria were chosen. That is, as shown in Fig. 3, the maximum difference of meniscus level (△H) should be less than 8.8 mm to ensure stable operation and quality. The velocity on the meniscus is also important. If the velocity is too low, the local freezing of the meniscus and hook formation [10, 11] may occur. On the other hand, abnormal high surface velocity leading to vortex formation [12, 13] and instability at the interface between the molten steel and slag [14-16], could entrain slag into the molten steel pool, resulting in both surface and internal defects in the final steel product. Therefore, maximum velocity (V_{max}) range of 0.1-0.38 m/sec is determined to be an optimal velocity range.

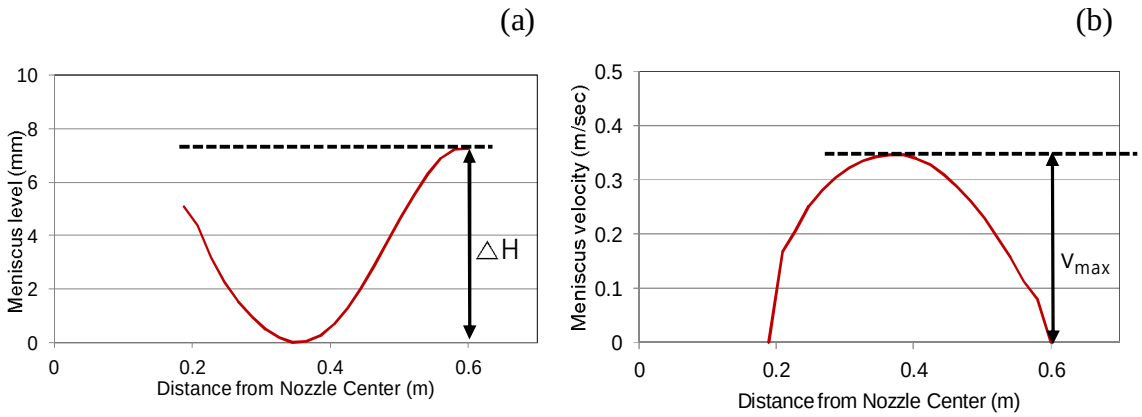

Fig. 3. Flow evaluation criteria, (a) maximum level difference (△H), (b) maximum meniscus flow velocity (V_{max})

3. Introduction of EMBr

Electromagnetic forces are applied to the flow field using EMBr . In order to effectively control the discharge from the SEN, we developed a U-shaped EMBr core as shown in Fig.3. The shape of the magnetic field differs from the popular ruler type design, as shown in Fig.4. By manipulating the shape of the curved field, the flow control can be optimized to be superior to that of a simple ruler type field.

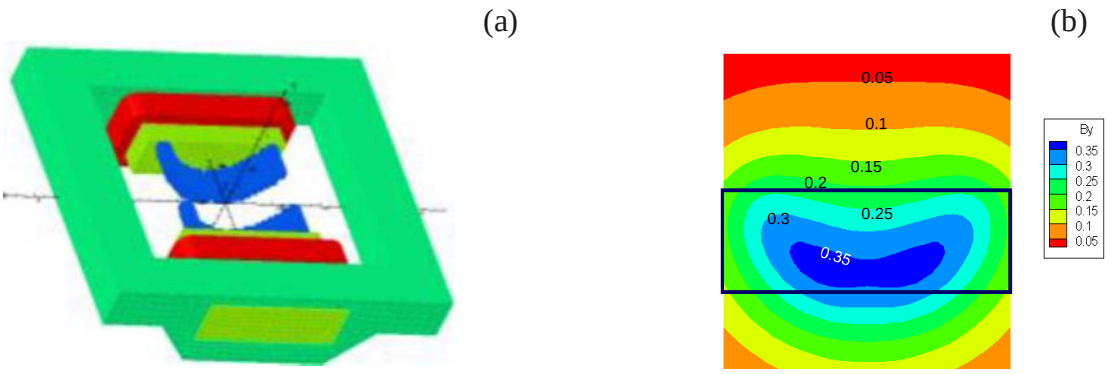

Fig. 4. Geometric configuration of CEM® EMBr, (a) schematic view, (b) magnetic field

In order to evaluate the present EMBr performance, calculations were carried out under conditions of a slab thickness of 90 mm, an average slab width of 1200 mm, and a casting speed of 6.5 m / min. This condition is conventional for currently performing endless rolling in CEM®. The magnetic field was set to 0.35T, obtained when the maximum current is applied. Figure 5 shows the computational results of the △H and V_{max} for the cases of with and without EMBr at each casting speed. When the EMBr is applied, △H is about 50%, and the speed is controlled to about 65% compared with the case without EMBr, respectively.

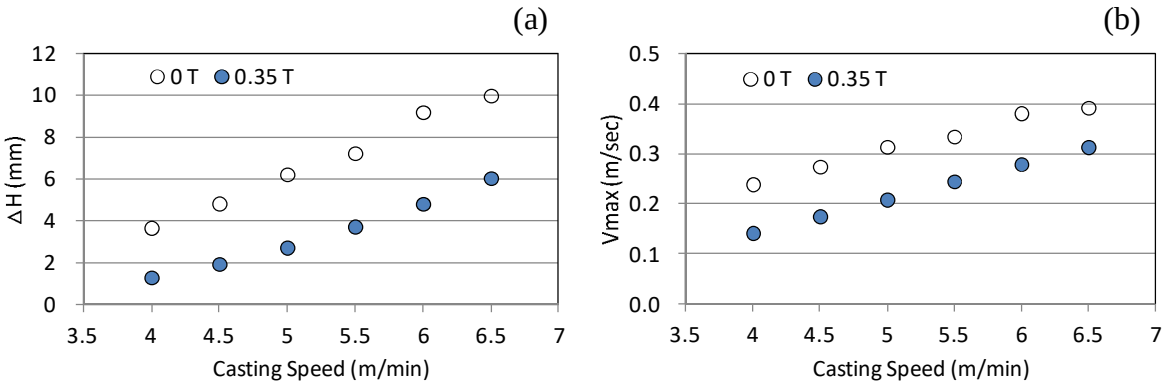

Fig. 5. Effects of casting speed and EMBr on: (a) △H, (b) V_{max}

4. Development of new SEN for High Throughput Operation

A new SEN was required to be developed for high throughput operation. The key technology is to increase the effective exit area of the SEN in order to decrease the velocity exiting the ports. In this study, we developed the new SEN design, which widens the cross sectional area by 50% compared with a conventional nozzle. Increasing the cross-sectional

area of the SEN ports is likely to increase the possibility of stress concentration on the outer wall of the SEN. This can be solved by optimizing the shape around the SEN port. As shown in Fig. 6, it can be seen that the stress of the new SEN is even smaller than that of the conventional one. Before conducting plant trials, the new SEN design was manufactured and it was confirmed that there are no serious problems in heat resistance by actually injecting molten steel into the SEN and performing a thermal shock test (Fig. 7).

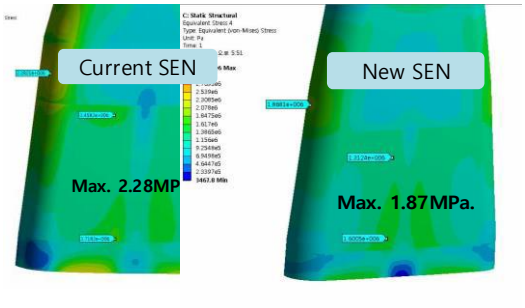

Fig. 6. Stress distribution

Fig. 7. Thermal shock test

Figure 8 shows the meniscus level profile from the nozzle center to the edge for the existing SEN and new SEN. Here, the dotted line indicates the case in which EMBr is not applied, and the solid line indicates the case with EMBr 0.35 T. In case of new SEN, it is found that the meniscus is controlled more effectively than the case of existing SEN, and EMBr is also a very useful tool for controlling the meniscus flow. Especially, if the new SEN is with applied U-shaped EMBr, △H can be controlled to about 30% of that with the current SEN without EMBr.

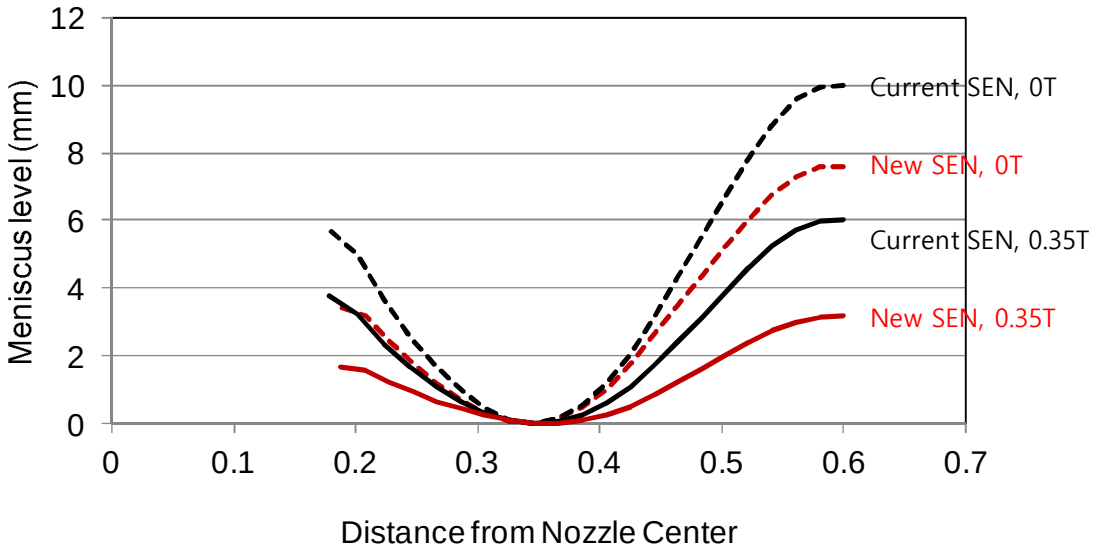

Fig. 8. Meniscus flow level of current SEN compared with new SEN, with and without EMBr

5. Plant Measurements and Model Validation

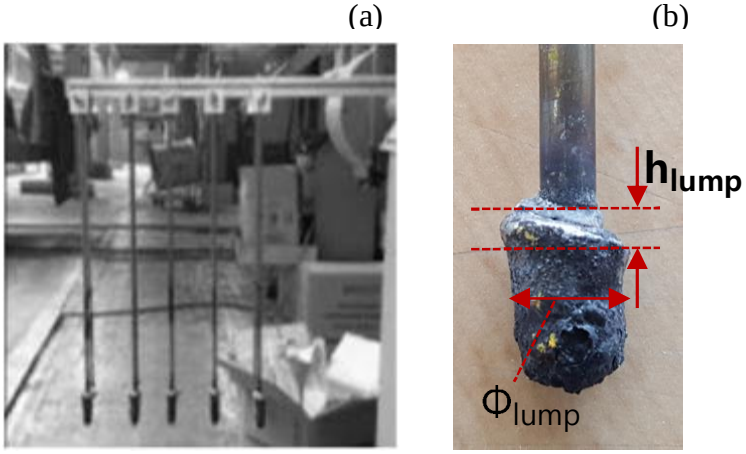

Fig. 9. Photos of the nail board test: (a) overview of nails, (b) lump solidified on a nail

Nail board dipping tests, which are commonly used for convenient plant measurement of the meniscus level and velocity at Posco, were carried out to validate the calculation results in this work. Specifically, two sets of measurements using 5 STS nails with 370 mm length and 5 mm diameter were conducted, as shown in Fig. 9. Details on this method to conduct these tests can be found in Rietow et. al's report [4]. If the lump height difference (h_{lump}) is measured as shown in Fig. 9 (b), surface velocity ($V_{surface}$) at each nail can be estimated from the following correlation [17] between h_{lump} and $V_{surface}$ in eq. (1), where and Φ_{lump} means lump diameter.

$$V_{surface} = 0.624 \cdot (\Phi_{lump})^{-0.696} \cdot (h_{lump})^{0.567} \qquad (1)$$

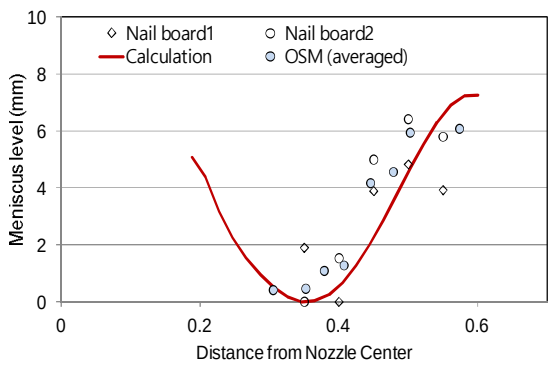

Fig. 10. Comparison of meniscus level : Calculation, nail board test and OSM

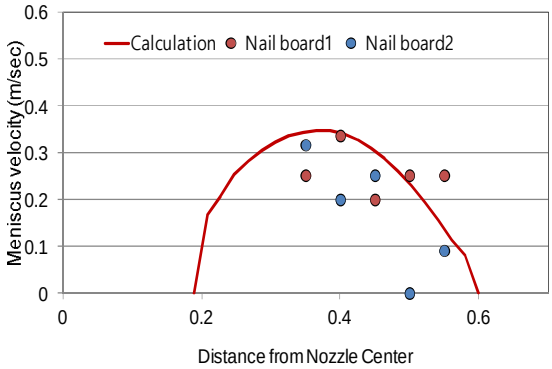

Fig. 11. Comparison of meniscus velocity : Calculation and nail board test

Figure 10 and 11 show the meniscus level and meniscus velocity distributions along the width direction from the center of SEN, respectively. The casting conditions are thickness 90

mm, width 1200 mm, casting speed 6.5 m/min and magnetic field 0.23 T using the new SEN. Figure 10 shows that the meniscus level is minimized in the middle region of the width direction. This is because the flow velocity of that part is maximized as shown in Fig. 11. Figure 10 represents the results of calculations are very consistent with those of the nail board tests and the averaged measured value of oscillation mark (OSM). The △H is less than 8mm, indicating a stable meniscus distribution. The meniscus velocity from the nail board tests is obtained using equation (1) and is in good agreement with the calculated results. Therefore, the numerical analysis used in this study is verified well. In particular, V_{max} is 0.35 m/sec, and we can expect stable in casting operation.

6. Effect of Electromagnetic field

If magnetic field is increased over a certain value, meniscus is dramatically stabilized. Figure 12 shows △H and V_{max} with magnetic field. When 0.35T magnetic field is applied, △H is reduced to 40% and V_{max} is reduced to 70%, compared with the case without EMBr.

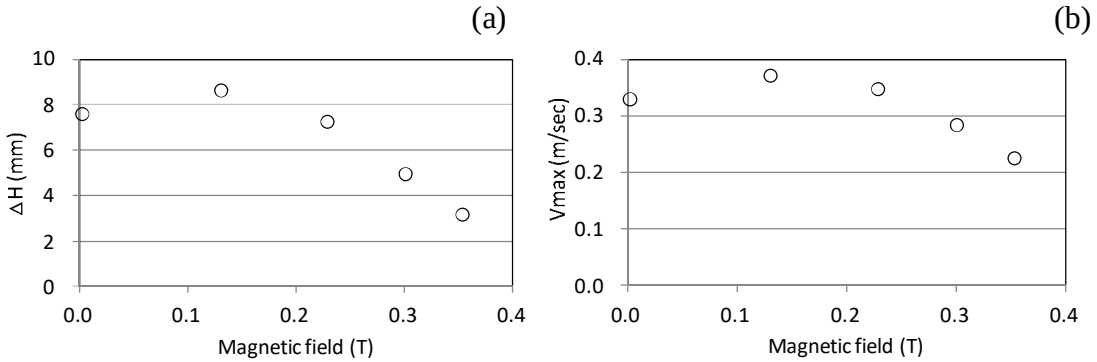

Fig. 12. Effect of magnetic field ; (a) △H, (b) V_{max}

Figure 13 shows velocity vectors and contours on the mid-section in the thickness direction when the magnetic field is applied with 0T and 0.35T. The red solid line represents the position of the EMBr core. The left side of the figure is the case without EMBr, where a secondary vortex with a large momentum is clearly observed compared to the right side of the figure with magnetic field 0.35T. One can notice that magnetic field make strong momentum diffusion happen, resulting in decrease of both △H and V_{max}.

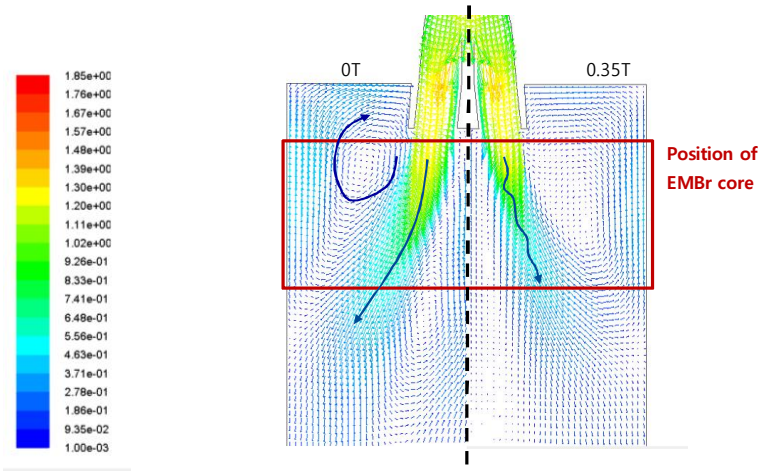

Fig. 13. Velocity vectors and velocity contours

7. Numerical Simulation for the High Mass Flow Condition

In this section, numerical simulations with high mass flow conditions are conducted. The new SEN combined with EMBr was applied to satisfy the two flow criteria mentioned in section. 2. Figure 14 shows the cases for the high throughput calculations conducted in this study on the plane of the casting width and thickness. In all cases, the casting speed is constant, that is, normal operating condition of 6.5 m / min. Case A is the current condition of CEM®; case B increases slab width to 1,600 mm; case C has slab width of 1,600 mm and thickness of 110 mm; and case D increases the width to 1,900 mm. Cases C and D correspond to super-high mass flow conditions of 8.4 and 8.7 ton/min.

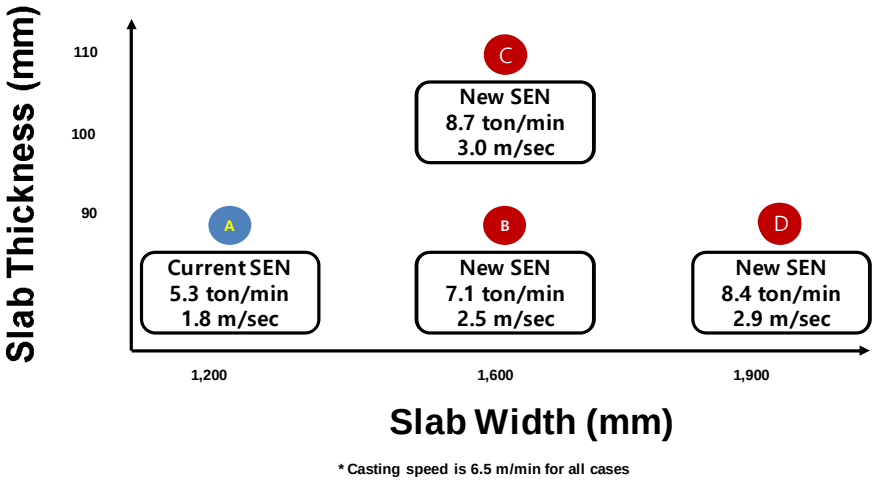

Fig. 14. Calculation cases for high mass flow condition

Figure 15 shows the △H and V_{max} for case C with the highest throughput. If the magnetic field is not applied, △H and V_{max} exceed the maximum criteria at 4.5 m/min. The meniscus velocity results are similar to those of △H. On the other hand, if EMBr is applied, it can be seen that there is no problem in either meniscus level or velocity.

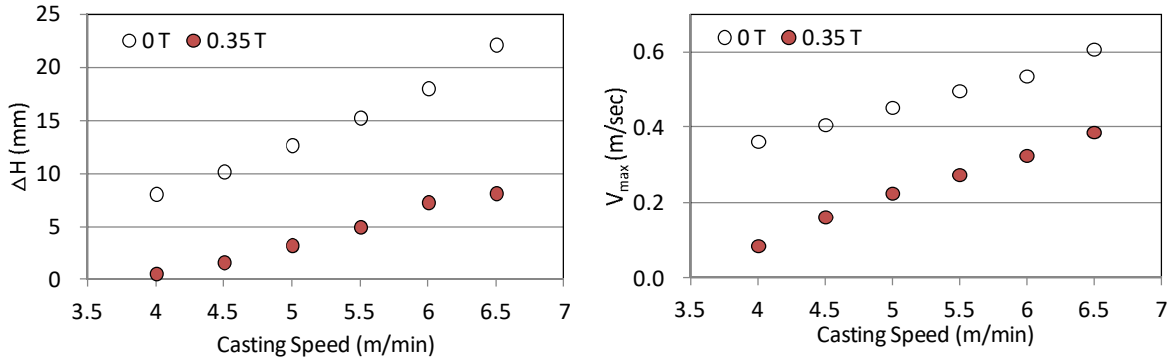

Fig. 15. Meniscus state for high throughput case C, (a) △H, (b) V_{max}

Table 1 shows calculated results of △H and V_{max} for all cases. In case A, stable operation can be expected regardless of EMBr operation, but in other cases, the situation is quite different. In case B, if EMBr is not applied, both △H and V_{max} are much beyond the criteria. The problems are even more serious for cases C and D, which have larger throughput. However, in all cases, if the EMBr is applied, stable operation can be expected.

Figure 16 shows velocity vectors and contours on the mid-section in the thickness direction when 0T and 0.35T magnetic fields are applied for various cases of high throughput. As shown in Table 1, when EMBr is not applied, the widest case D shows that a strong secondary vortex is formed and △H and V_{max} are greatly increased. On the other hand, when the EMBr effect is maximized, it can effectively diffuse the jet momentum and the meniscus becomes stable for case D.

Table 1 Result of calculation

case	width (mm)	thickness (mm)	magnetic field (T)	throughput (ton/min)	ΔH (mm)	V_{max} (m/sec)
caseA-1	1200	90	0.00	5.34	7.6	0.33
caseA-2	1200	90	0.35	5.34	3.2	0.23
caseB-1	1600	90	0.00	7.11	19.33	0.57
caseB-2	1600	90	0.35	7.11	4.12	0.28
caseC-1	1600	110	0.00	8.69	22.13	0.61
caseC-2	1600	110	0.35	8.69	8.14	0.39
caseD-1	1900	90	0.00	8.45	34.13	0.79
caseD-2	1900	90	0.35	8.45	4.78	0.29

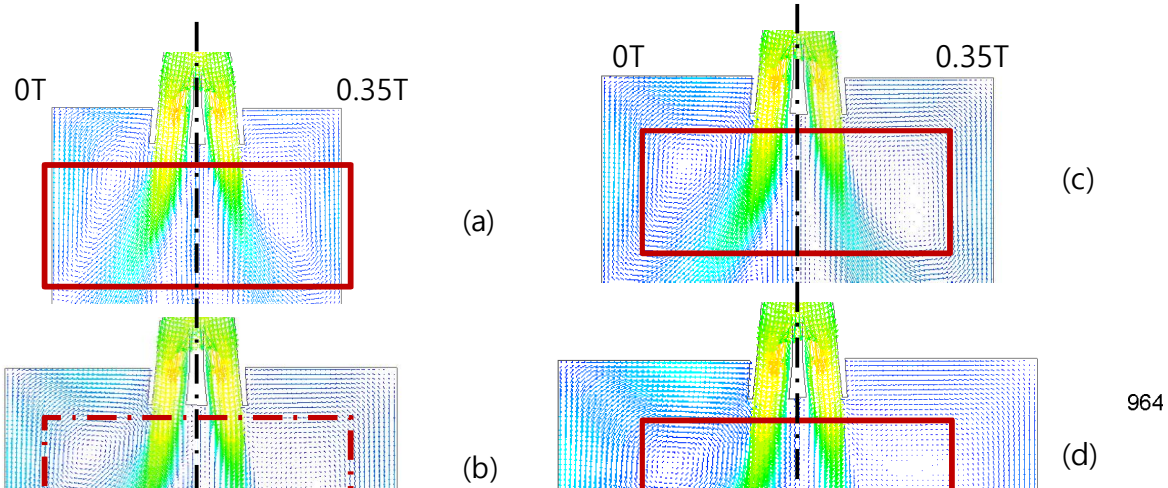

8. Conclusion

In this study, numerical analysis of mold flow was performed for high throughput conditions, which are 45% larger than that used for the CEM® casting process currently in operation. A new SEN for high throughput was designed and investigation was conducted to evaluate the meniscus level and velocity combined with EMBr. A key technology of the new SEN is to increase the exit area in order to decrease the exit velocity. The port area of the new SEN is increased by 50% compared with that of a conventional nozzle. In order to validate the numerical method and results, the meniscus level and velocity from plant measurements using nail board tests were obtained. Those tests are in good agreement with the calculated results.

If electromagnetic field is increased over a certain level, the meniscus is dramatically stabilized. With this knowledge, numerical simulations were conducted for several high mass flow cases, and it was found that using the new SEN combined with the current U-shaped EMBr design, stable meniscus level and velocity can be expected without any serious problems.

References

[1] J.-Y. Hwang, S.-H. Lee, S.-Y. Kim and M.-C. Shin, Characteristics of heat transfer in the high speed casting up to 8.0 m/min, METEC 2015, (2015, Dusseldof, Germany)

[2] A. Lehman, Electromagnetic braking improves steel quality in continuous casting, ABB Review 1 (1996), p.4

[3] B. G. Thomas and R. Chaudhary, State of the art in electromagnetic flow control in continuous casting of steel slabs : modeling and plant validation, 6th Int. Conf. Elecromagnetic Processing of Materials EPM (2009)

[4] B. Rietow and B. G. Thomas, Using nail board experiments to quantify surface velocity in the CC mold, AISTech 2008, (2008, Pittsburgh, USA)

[5] V. Norbert, O. Hans-Jurgen and R. Markus, Fluid flow in continuous casting affected by magnetic fields, 8th ECCC, Dusseldorf (2014)

[6] S.-M. Cho, S.-H. Kim and B. G. Thomas, Transient Fluid Flow during Steady Continuous Casting of Steel Slabs: Part I. Measurements and Modeling of Two-phase Flow, ISIJ Int. (2014, Vol. 54, No. 4), p. 845

[7] S.-M. Cho, S.-H. Kim and B. G. Thomas, Transient Fluid Flow during Steady Continuous Casting of Steel Slabs: Part II. Effect of Double-Ruler Electro-Magnetic Braking, ISIJ Int. (2014, Vol. 54, No. 4), p. 855

[8] R. Singh, B. G. Thomas and S. P. Vanka, Large Eddy Simulations of Double-Ruler Electromagnetic Field Effect on Transient Flow During Continuous Casting, Metallurgical and Materials Trans. B (2014, Vol. 45B), p. 1098

[9] M. J. Cho, Discretization of Lorentz force term, Numerical Heat Transfer (2006, Part B, 49), p.599
[10] J. Sengupta, B. G. Thomas, H. Shin, G. Lee and S. Kim: *Metall.Mater. Trans. A*, 37A (2006), 1597.
[11] H. Shin, S. Kim, B. G. Thomas, G. Lee, J. Park and J. Sengupta: *ISIJ Int.*, 46 (2006), 1635.
[12] S-M. Cho, G-G. Lee, S-H. Kim, R. Chaudhary, O-D. Kwon and B. G. Thomas: Proc. of TMS 2010, TMS, Warrendale, PA, USA, (2010), 71.
[13] S-M. Cho, S-H. Kim, R. Chaudhary, B. G. Thomas, H-J. Shin, W-R. Choi and S-K. Kim: *Iron Steel Technol.*, 9 (2012), 85.
[14] M. Iguchi, J. Yoshida, T. Shimizu and Y. Mizuno: *ISIJ Int.*, 40 (2000), 685.
[15] L. C. Hibbeler, R. Liu and B. G. Thomas: Proc. of 7th ECCC, METECInSteelCon, Steel Institute VDEh, Dusseldorf, Germany, (2011).
[16] R. Hagemann, R. Schwarze, H. P. Heller and P. R. Scheller: *Metall. Mater. Trans. B*, 44B (2013), 80.
[17] R. Liu, J. Sengupta, D. Crosbie, S. Chung, M. Trinh and B. Thomas: Proc. of TMS 2011, TMS, Warrendale, PA, USA, (2011).